buildings

MDPI

Article

Applicability of Vegetation to Reduce Traffic-Borne PM2.5 Concentration in Roadside User Zones in Hot Arid Climates: The Case of Central Doha, Qatar

Soujanya Mogra * and Mohd Faris Khamidi

Architecture and Urban Planning Department, College of Engineering, Qatar University, Doha P.O. Box 2713, Qatar; mohd.khamidi@qu.edu.qa
* Correspondence: sm1513220@student.qu.edu.qa

Abstract: The 'Beautification of Roads and Parks in Qatar' is an urban development project that intends to provide space for exercising in roadside greenery in central Doha due to a lack of accessible open spaces. Considering the potential health risks associated with inhaling traffic-borne PM2.5, this study investigated the efficacy of four common road vegetation scenarios in reducing traffic-borne PM2.5 concentration in roadside user zones using ENVI-met. It examined Spearman's rank correlation between air temperature, relative humidity, traffic emission rate, and PM2.5 concentration in roadside user zones. Based on the results, (1) hedgerows lower PM2.5 concentrations in roadside user zones, while trees significantly increase the concentration. (2) There is a strong association between air temperature and relative humidity and the PM2.5 concentration. The PM2.5 concentration decreases as air temperature increases but it increases as relative humidity increases. (3) There is a moderately negative association between the traffic emission rate and the PM2.5 concentration; however, this association is not found to be statistically significant. The ENVI-met simulation showed a slight overestimation of PM2.5 concentration compared to the wind tunnel simulation. These findings provide insight into planning road vegetation to reduce traffic-borne PM2.5 in roadside user zones in the local hot arid climate.

Keywords: road vegetation; traffic-borne PM2.5; meteorological conditions; Spearman's rank correlation; ENVI-met

Citation: Mogra, S.; Khamidi, M.F. Applicability of Vegetation to Reduce Traffic-Borne PM2.5 Concentration in Roadside User Zones in Hot Arid Climates: The Case of Central Doha, Qatar. *Buildings* **2024**, *14*, 1388. https://doi.org/10.3390/buildings14051388

Academic Editors: Xia Zhang and Hui He

Received: 20 March 2024
Revised: 26 April 2024
Accepted: 2 May 2024
Published: 13 May 2024

1. Introduction

Air pollution is a significant environmental threat to human health. Today, 99 percent of the world's population inhales poor air [1]. Qatar is one of the countries with the highest ambient PM2.5 concentrations [2]. PM2.5 refers to fine particulate matter with a diameter of 2.5 microns or less and is a commonly used standard measurement of outdoor air quality [3]. The annual average PM2.5 in urban Qatar in 2023 is classified between 'moderate' to 'unhealthy for sensitive groups' that range between 12.1 and 55.4 $\mu g/m^3$, which is higher than the 'good' classification of the United States Environmental Protection Agency (EPA) guidelines [4,5]. Studies have revealed that road vehicular traffic is one of the dominant sources of particulate matter pollution in Doha [6–8]. The literature shows that the canyon-like configuration of buildings along urban roads, known as street canyons, impedes the dispersion of pollutants emitted by traffic and increases road users' exposure to the pollutants [9,10]. Hence, densely built urban areas are more vulnerable to traffic-borne air pollution.

Implementing vegetation along urban roads is a passive strategy to reduce roadside users' exposure to traffic-borne air pollutants [9,11]. Vegetation reduces traffic-borne PM2.5 exposure via absorption, dispersion, and deposition mechanisms [12]. It diverts the pollutants' stream from the source away from the roadside user zone via dispersion. Vegetation

filters the pollutant particles through the leaves and branches before reaching the pedestrians via deposition. The leaves and bark absorb gaseous pollutants and fine particulate matter. Figure 1 is a graphical presentation of traffic-borne pollution dispersion, deposition, and absorption by road vegetation. However, road vegetation can increase traffic-borne air pollution exposure for roadside users if not carefully aligned with the dispersion and deposition mechanisms. For example, trees can block vertical air exchange and increase the pollutant concentration in street canyons [13,14]. Therefore, road vegetation planning is crucial to reducing roadside users' exposure to traffic-borne pollutants.

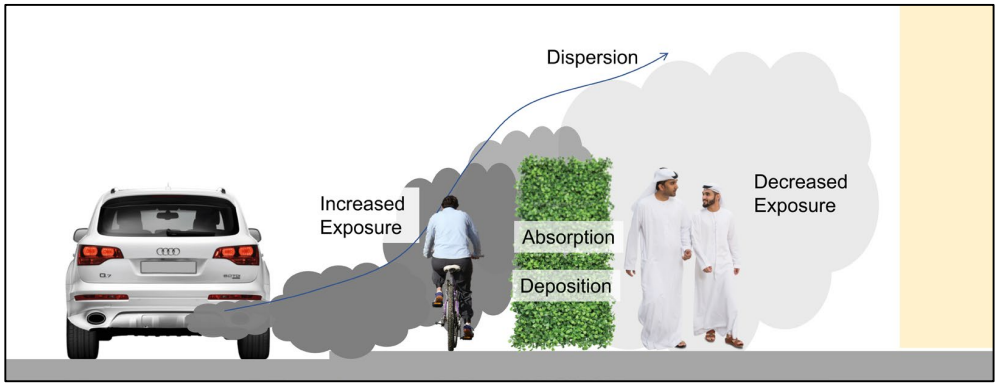

Figure 1. A graphical representation of street vegetation mechanisms in the reduction in traffic-borne pollutant exposure.

Various factors, such as wind conditions, air temperature, relative humidity, road geometry, traffic emission rate, and the physical characteristics of the vegetation, govern the dispersion of pollutants by road vegetation [9,11]. In particular, these wind directions are thought to have different flow fields. For example, Table 1 shows studies that looked at how plants affected pollutant levels in street canyons when the wind came from 90°, 45°, or 0° to the street's main axis.

Buccolieri et al. [13] investigated the influence of avenues like tree planting pollutant concentration in a street canyon with a height (H) to width (W) ratio of 1 (H/W = 1). The findings showed that the average concentration of pollution on the leeward side of the wall increased significantly for perpendicular approaching wind in comparison to obliquely approaching wind to the main axis of the street. Conversely, an investigation by Gromke and Ruck [14] on avenue-like tree planting showed the highest concentration along the leeward wall of a street canyon, with an aspect ratio (H/W) of 0.5 for oblique wind compared to perpendicular approaching wind. A study by Y.-D. Huang et al. [15] looked at seven wind directions with equal gaps between 0° and 90°. It found that the average wall and maximum wall concentrations were highest on the leeward side for 75° approaching wind in a long street canyon, which means that the length (L) to height (H) ratio was more than seven. Overall, the literature showed that street canyons with orientations of 45° and 75° to the direction of the prevailing wind significantly degrade the air quality in the roadside user zone.

Several studies, including Li et al. [16], Jia Wanga et al. [17], Zhu et al. [18], and Wania et al. [19], have investigated the influences of wind speed on vegetation-induced pollutant exposure reduction. Researchers discovered that wind speed has a significant influence on vegetation pollutant concentration, particularly on obliquely oriented urban roads facing the prevailing wind direction [20]. On the other hand, researchers found that wind speed had less of an influence on the vegetation effect on perpendicularly oriented urban roads [16]. Therefore, it is crucial to explore the impact of vegetation on pollutant concentration in roadside user zones of urban roads oriented at an oblique angle to the wind, as it significantly affects the exposure of roadside users to traffic-borne pollutants.

Trees and hedgerows are commonly considered for pollutant exposure reduction studies in roadside areas, as shown in Table 1. Zhang et al. [20] discovered that sideways

shrub arrangements work well for urban roads oriented parallel and oblique to the wind. However, wind angles other than 45° to the main axis of the canyon-like urban roads are rarely considered in the literature. This can provide a deep understanding of how to apply suitable vegetation scenarios for pollutant concentration reduction in roadside user zones.

Table 1. Summary of the literature on the effect of vegetation on traffic-borne pollutants' concentration in street canyons for various wind conditions.

Researchers	Wind Directions	Wind Speed [m/s]	Aspect Ratio [H/W]	Vegetation Configurations
Gromke and Ruck [21]	90°	4.65	1	Trees
Buccolieri et al. [13]	90°	4.7	0.5	Trees
Li et al. [16]	90°	1, 2, 3, 20	0.39, 0.18, 0.78	Trees and vegetation barriers
Jia Wanga et al. [17]	90°	1, 3	0.5, 0.9, 1.2	Vegetation barriers
Huang et al. [22]	90°	4.7	0.5	Trees
Zhang et al. [23]	90°	4.7	0.5	Trees
Zhu et al. [18]	90°	2.45, 6.7, 9.35	0.6, 0.67, 1, 2	Trees
Shen et al. [24]	90°	4.7	0.5	Trees, hedgerows, and Tree-hedge
Buccolieri et al. [25]	90°, 45°	4.7	0.5, 1	Trees
Wania et al. [19]	90°, 45°	1, 3	1	Hedgerows and trees
Vos et al. [26]	90°, 45°	3	Asymmetrical	Trees, hedgerows, and green barriers
Morakinyo and Lam [27]	90°, 45°	1, 3	1, 2, 3, 4	Trees
Amorim et al. [28]	45°, 0°	4–7, 5–10	0.33, 0.75	Trees
Gromke et al. [29]	90°, 0°	4.65	0.5	Hedgerows
Hong et al. [30]	90°, 0°	3	0.5, 1, 2	Trees
Gromke and Ruck [14]	90°, 45°, 0°	4.65	0.5, 1	Trees
Zhang et al. [20]	90°, 45°, 0°	4.7, 2	0.5	Trees, hedgerows, tree-hedgerow combinations

Most of the studies are concentrated on the Koppen Climate classifications (Cfb), which indicate a temperate climate with warm summers but no dry season. It includes Buccolieri et al. [13], Buccolieri et al. [25], Chen et al. [31], Gromke et al. [29], Gromke and Ruck [14,21], and Vranckx et al. [32]. Amorim et al. [28] conducted some studies in regions with hot dry summers and moderate wet winters (CSa); Li et al. [16] conducted a few studies in a warm temperate climate region (Cfa); Hong et al. [30] and Wania et al. [19] conducted certain studies in a humid continental climate (Dwa); and Zhu et al. [18] conducted a few studies in a warm and temperate climate region.

Most of the previous studies have investigated the thermal effect of street canyon surfaces on pollutant dispersion [33–36]. Only Chen et al. [31] examined the influence of relative humidity on particulate matter pollutant reduction by open road vegetation in Wuhan, China, in a field experiment. The study revealed that relative humidity has the most influence on pollutant removal by road vegetation compared to wind speed and air temperature. Due to hygroscopic particles increasing in size when they absorb water, which affects their deposition, it is important to consider the influence of the relative humidity. There is a lack of literature on the effects of urban roadside vegetation on roadside users' exposure to traffic-borne pollutants in street canyons in hot arid climate (BWh) regions, where Qatar is located. This study aims to investigate the impact of BWh climatic conditions on the relationship between road vegetation and traffic-related PM2.5 concentrations in roadside user zones in Doha, Qatar.

In addition, it is crucial to determine the relationship where the presence of vegetation will impact the pollutant concentration due to the traffic emission rate. Based on this relationship, vegetation scenarios can be implemented according to the road hierarchy. Chen et al. [31] previously demonstrated, in the context of open roads, that major roads suit shrubs and small trees, sub-arterial roads suit shrubs and grass, and branch roads prefer parallel trees. However, there are no studies that have investigated the association between traffic emission rate and pollution concentration in the roadside user zone in the presence of vegetation on canyon-like urban roads.

A recent pilot survey conducted by Mogra et al. [37] in central Doha revealed that aesthetic enhancement of streets, micro-climate regulation, and air quality enhancement benefits from road vegetation are highly preferred by roadside users. Roadside users most prefer trees because they perceive them to provide shade. People perceive hedgerows as enhancing the safety of children and pets. Qatar Urban Design Compendium [38] also considers trees an integral element of the streetscape in local hot and arid climatic conditions. In this regard, four common road vegetation scenarios, i.e., center hedgerows (CH), sidewise hedgerows (SH), center trees (CT), and sidewise trees (ST), are considered.

Researchers extensively use Computational Fluid Dynamics (CFD) to evaluate the effects of vegetation on pedestrians' exposure to traffic-borne pollutants. A few studies by Wania et al. [19], Vos et al. [26], Morakinyo and Lam [27], and Jia Wanga et al. [17] adopted ENVI-met numerical simulation. ENVI-met, unlike general CFD tools, specifically designs itself for microscale modeling of urban and environmental meteorology. Analyzing air interaction within and between vegetation, surfaces, and buildings is a specific application of ENVI-met. Moreover, ENVI-met has a built-in traffic tool that automatically calculates traffic emission rates based on annual average daily traffic (AADT). A study by Sun et al. [39] showed that ENVI-met performs better compared to the most frequently used CFD software, ANSYS Fluent, in assessing the correlation between PM concentrations and intersectional and meteorological factors. Therefore, this study employs ENVI-met to examine the impact of four common urban road vegetation scenarios on the exposure of roadside users to traffic-borne PM2.5.

This study seeks answers to the following research questions:

1. What are the effects of the four vegetation scenarios, i.e., CH, SH, CT, and ST, on traffic-borne PM2.5 concentrations in the roadside user zone in comparison with the base case scenario?
2. How are variables like air temperature, relative humidity, and traffic emission rate correlated to traffic-borne PM2.5 concentrations in roadside user zones?

2. Materials and Methods

2.1. Conceptual Framework

This study is based on a numerical simulation. The research parameters include both environmental and built features. The main variables under investigation are air temperature, relative humidity (RH), traffic emission rate, and vegetation. Other parameters are the traffic emission rate, wind speed, wind direction, and road geometry. As shown in Figure 2, the conceptual framework includes collecting data, making models, validating them, and evaluating four vegetation scenarios. It also looks at how meteorological variables and traffic emission rate affect PM2.5 reduction at roadside user zones when vegetation is present, in order to learn more about how to plan vegetation for urban roads.

2.2. The Site

Four-ring roads with a concentric street pattern encircle central Doha. The arterial roads radiate from the center area. The center area is the densest area of Doha in terms of the resident population [40]. Bank Street and Ali Bin Abi Talib Street in central Doha were chosen as case study sites. The meteorological data were observed at the Old Doha Airport weather station, the nearest weather station to the two sites. The locations of the two sites relative to the weather station are shown in Figure 3A.

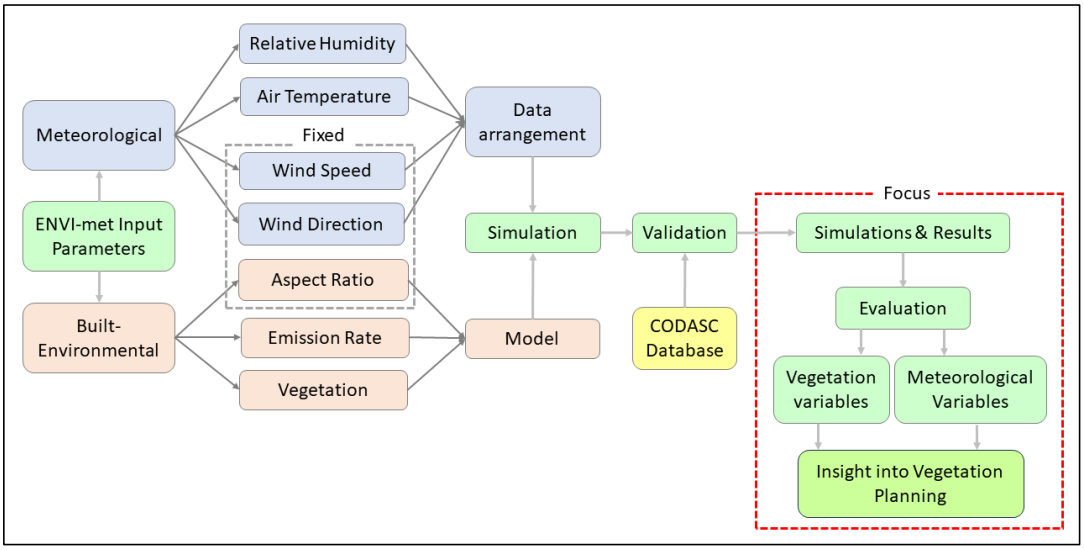

Figure 2. A conceptual framework for the evaluation of urban road vegetation scenarios to reduce roadside users' exposure to traffic-borne PM2.5 exposure.

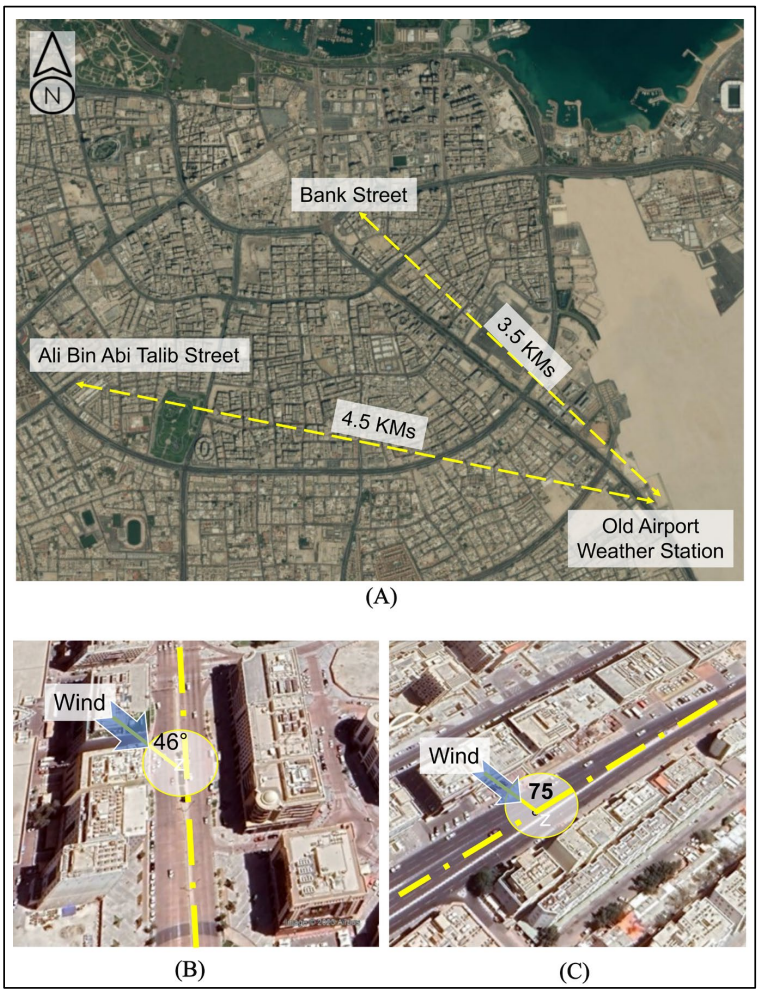

Figure 3. Locations of the sites and the weather station on the map of central Doha (**A**). Images of Bank Street (**B**) and Ali Bin Abi Talib Street (**C**). Source: Qatar GIS Portal and Google Earth. Accessed on 29 October 2023.

The sites were chosen according to aspect ratio and orientation to the prevailing wind direction. Both sites have an identical aspect ratio of approximately 0.43. The prevailing wind direction in central Doha is 310° north-facing. The first road selected for this study, as shown in Figure 3B, is Bank Street, consisting of buildings with heights between 28 and 30 m on both sides, each almost six meters apart. The road has a width of approximately 66 m. The orientation of the first road is 266° north-facing, which is 46° in the wind direction. Secondly, Ali Bin Abi Talib Street, as shown in Figure 3C, consists of building heights between 17 and 21 m on both sides, except for the leeward corner building, which has a height of 12 m. The road has a width of 41 m. For this case, road orientation is 235° north-facing, i.e., 75° to the prevailing wind direction. Both sites are six-lane traffic roads.

2.3. ENVI-Met Modeling

This study used ENVI-met software to examine the effects of urban road vegetation on traffic-borne PM2.5 concentrations in roadside user zones. The numerical description of ENVI-met can be found at Bruse [41]. The ENVI-met model was validated using the CODASC database for an idealized street canyon scenario with an aspect ratio of 0.5.

2.3.1. ENVI-Met Validation

ENVI-met model performance for an idealized street canyon was validated using the CODASC (Concentration DAta of Street Canyons) data. Several researchers, including Abhijith and Gokhale [42], Buccolieri et al. [43], Jeanjean et al. [44,45], and Morakinyo and Lam [27] have used CODASC to validate their study. CODASC data are developed in the Laboratory of Building and Environmental Aerodynamics at the Institute for Hydromechanics (IfH) at the University of Karlsruhe, Germany, through a series of wind tunnel experiments. It provides a normalized pollutant concentration distribution at street canyon walls. Each wall of the street canyon has 700 grid points of normalized concentration measurement at positions x+ = 0.04167 x/H. 4. Figure 4 shows the x, y, and z axes of the street canyon. More details are on the CODASC webpage [46].

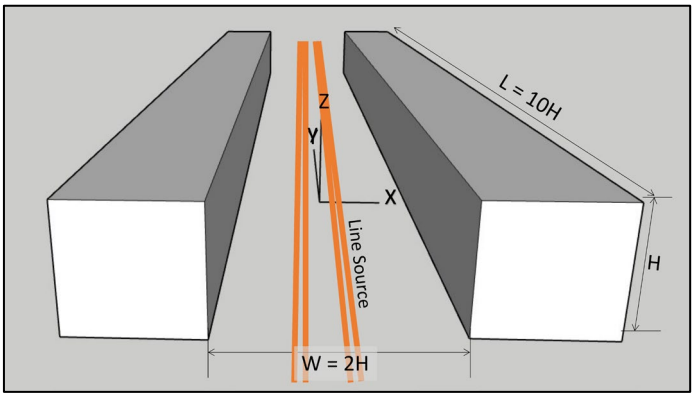

Figure 4. The axis x, y, and z of the street canyon. Source: CODASC database webpage (Re-drawn).

The ENVI-met model performance showed a slight overestimation of the PM2.5 concentration for the base-case scenario, with a FB value of 0.49. However, in the case of the vegetation scenario, the FB value was within the acceptable range (<|0.3|). This study applied a grid resolution of 3.6 m × 3.6 m × 2 m. Previously, a study by Morakinyo and Lam [27] considered a grid resolution of 0.5 m × 0.5 m × 0.5 m. The study revealed an overestimation of PM2.5 concentration for both the base-case scenario and the scenario with trees with FB values of 0.5 and 0.8, respectively.

ENVI-met student license version 5.5.1 is used in this study. A cartesian resolution of 3.6 m × 3.6 m × 2 m was used in ENVI-met modeling. ENVI-met 3D models of street canyons with an aspect ratio of 0.5 were generated, both with and without tree planting,

like the models used in wind tunnel experiments to develop CODASC data. Figure 5 shows the sections of the wind tunnel street canyon models, both without and with tree planting.

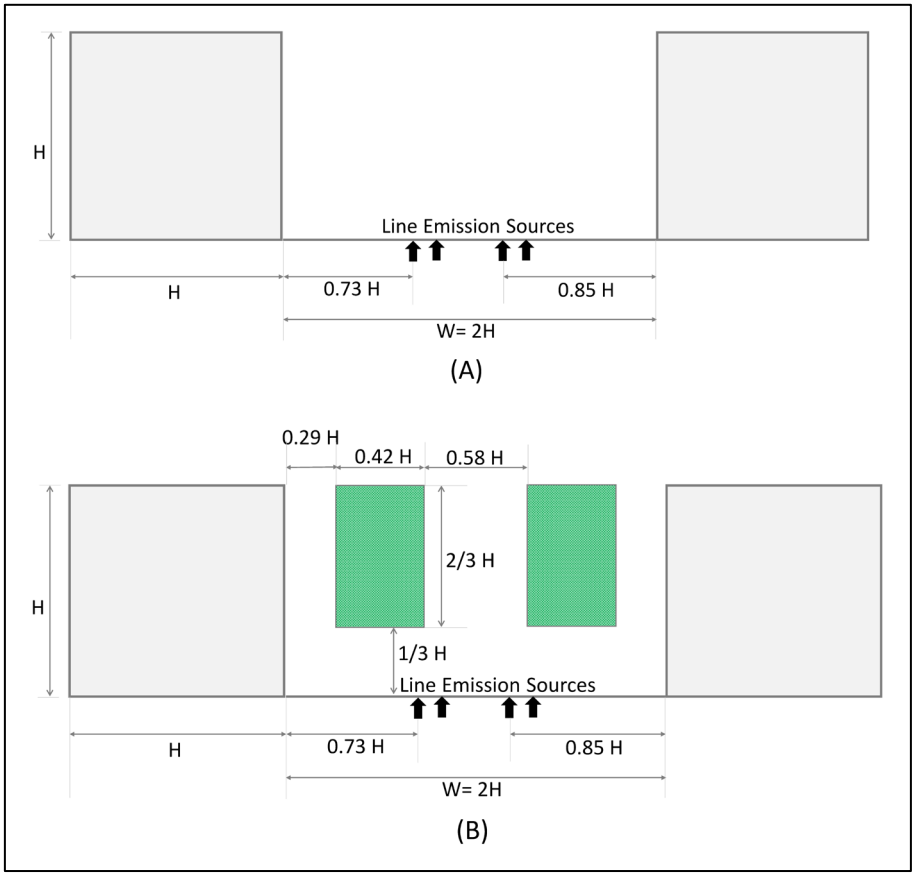

Figure 5. Sections of the wind tunnel experiment model the street canyons with an aspect ratio of 0.5 without trees (**A**) and with trees (**B**). Source: CODASC, KIT (Re-drawn).

The ENVI-met model replicated the wind tunnel model with a building height and width of 18 m. The distance between the buildings was set to 36 m to match the aspect ratio of 0.5. The line emission sources in the ENVI-met models were positioned to closely align with the locations of line emission sources in the wind tunnel experiment models. The porosity of the trees in the wind tunnel experiment model is 96.0%. The leaf area density (LAD) of 1.5 m^2 m^{-3} was used in the ENVI-met tree modeling to correspond with the porosity of the wind tunnel's tree model. Ten nested grids were implemented for the models. Plans of the ENVI-met model layouts are provided in Supplementary Figures S1 and S2.

The selected sites for this study have an oblique orientation to the prevailing wind direction. Hence, to investigate ENVI-met model performance, a CODASC dataset on wind direction 45° to the street axis was considered. The wind speed used in the wind tunnel experiment is 4.7 m/s at the building roof height, i.e., 18 m. The annual average wind speed in central Doha is 3.76 m/s, measured at a 10-m height, which is 4.7 m/s at a height of 18 m above the ground. Meteorological data input for the ENVI-met model was provided in Table 2 in Section 2.3.3 and Table S1.

Table 2. Normalized pollutant concentration at the street canyon walls when oriented at 45° to the wind direction.

BOOT Criteria	Ideal Range	Acceptable Range	Base Case Model	Model with Trees
NMSE	0	<1.5	0.27	0.03
R	1	>0.8	0.995	0.966
FA2	1	>0.5	1	1
|FB|	0	<|0.3|	0.49	−0.156

The PM2.5 concentration data of ENVI-met models were extrapolated from all 13 vertical and 50 horizontal grid points at both walls of the street canyons. The PM2.5 concentration data obtained from ENVI-met simulations were normalized using the following formula:

$$C^{+} = [C \times U_H \times H]/Q_1 \quad (1)$$

where H is the height of the building, Q_1 is the intensity of the PM2.5 emission line source, which is a uniform line emission of 15 µg/s, U_H is the wind speed at height H, C is the PM2.5 concentration at the grids, and C^{+} is the normalized concentration at the grids.

Chang and Hanna [47] developed a statistical analysis tool (known as BOOT) to evaluate pollutant dispersion modeling of the street canyons. The ASTM (American Society for Testing and Materials) procedure was used to evaluate the ENVI-met model's performance using BOOT software. The BOOT has four criteria for model acceptance: NMSE Normalized Mean Squared Error (NMSE), correlation coefficient (R), Fractional Absolute Error 2 (FA2), and Absolute Fractional Bias (FB). Table 2 refers to a street canyon with an aspect ratio (H/W) of 0.5, with and without avenue trees.

Table 2 shows that for the base case model, the NMSE, R, FA2, and FB values are 0.27, 0.995, 1, and 0.49, respectively. The model slightly overestimated the pollutant concentration. Previously, a performance evaluation of an ENVI-met model for a street canyon with an aspect ratio of 1 and a grid resolution of 0.5 m × 0.5 m × 0.5 m based on CODASC by Morakinyo and Lam [27] also showed an overestimation of the pollutant concentration. For the model with avenue trees, the NMSE, R, FA2, and FB values are 0.03, 0.966, 1, and −0.156, respectively, all within the acceptable range.

Overall, the ENVI-met models of the base case and avenue, like the tree planning case, were in reasonable agreement with the wind tunnel experiment of the CODASC database. Therefore, this study applied a grid resolution of 3.6 m × 3.6 m × 2 m for the site models.

2.3.2. Model Scenarios

The ENVI-met models of the two case study sites included five scenarios: base case, center hedgerow (CH), sidewise hedgerow (SH), center trees (CT), and sidewise trees (ST). Figure 6 presents 3D views of the site models. The base case is the scenario before vegetation implementation.

In the CT and ST scenarios, the height and width of the tree models are 10 and 7 m, respectively, with a spherical crown of leaf area density (LAD) of 1.5 m^2 m^{-3}. In the CH and SH scenarios, the height and width of the hedgerows are two and one meters, respectively, with a LAD of 3 m^2 m^{-3}. The vegetation models were created in Albero with a grid resolution of 1-m × 1-m × 1-m and then imported to the models with a grid resolution of 3.6-m × 3.6-m × 2-m.

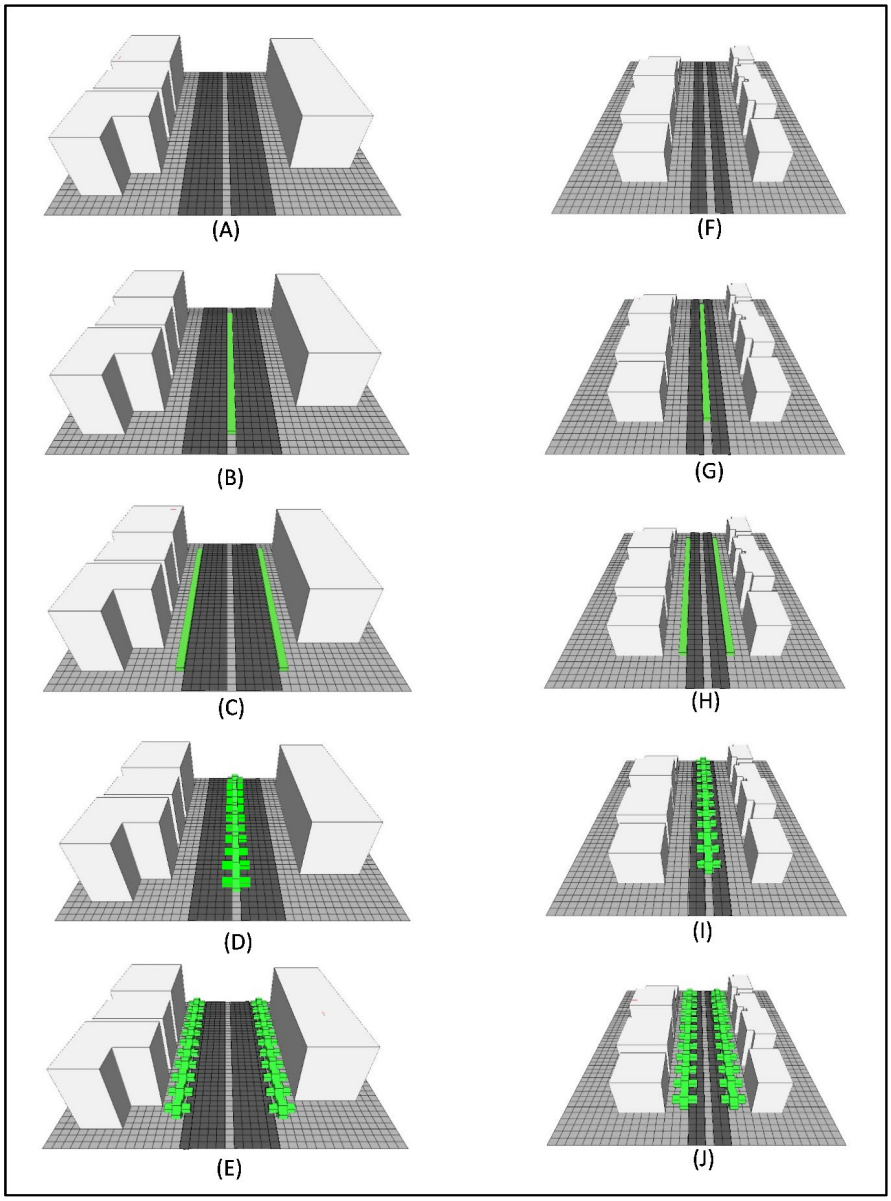

Figure 6. ENVI-met models of the five scenarios, i.e., (**A**–**E**) are respectively for Base Case, Centre Hedgerow (CH), Sidewise Hedgerows (SH), Centre Trees (CT), and Sidewise Trees (ST) scenarios of Bank Street (**left**) and (**F**–**J**) are, respectively, for Base Case, Centre Hedgerow (CH), Sidewise Hedgerows (SH), Centre Trees (CT), and Sidewise Trees (ST) scenarios of Ali Bin Abi Talib Street (**right**).

2.3.3. Meteorological Data Collection and Input

The meteorological dataset was extrapolated from Iowa Environmental Management (IEM) [48]. Observations recorded at Old Doha Airport from midnight on 1 January 2016 to midnight on 1 January 2022 on wind speed, air temperature, relative humidity, and specific humidity at 2500 m were considered. Averaged hourly data from 12 a.m. to 10 p.m. for relative humidity (RH), air temperature, and specific humidity at 2500 m were calculated. The prevailing wind direction of the six-year-old, which is 310° north-facing, and the yearly average wind speed of 3.76 m/s were used.

The performance simulation of the ENVI-met model commenced at zero hours and continued for six hours, concluding at 6 a.m. The PM2.5 concentration output values from the sixth hour were utilized. Typically, the initialization time and the initial six hours are

required to establish atmospheric stability; therefore, they are disregarded. Table 3 shows the meteorological data input.

Table 3. Meteorological data input for the ENVI-met simulation file.

Input Parameters	Values	Attributes
Wind Speed at a height of 10-m	3.76 m/s	Fixed
Wind direction	310° North bearing	Fixed
Specific humidity in 2500 m	12.9 g/kg	Fixed
Relative humidity (RH) in percentage (%)	Hourly average	Variable (Supplementary Table S1)
Air temperature in Celsius°	Hourly average	Variable (Supplementary Table S1)

2.3.4. Traffic Emission Rate Calculation and Input

During the time of this study, annual average daily traffic (AADT) of the case study roads was not readily available. Therefore, the Transportation Research Board'sthe Highway Capacity Manual, 6th Edition was referred. The manual considers AADT between 29,100 and 55,300 vehicles per day as a rule of thumb for a six-lane urban road with signals [49]. As a result, we assumed that a six-lane traffic road with three lanes in each direction, left turn lanes at busy intersections, and coordinated signals would have an AADT of 55,300 vehicles per day.

Hourly traffic emission rates at a height of 0.5 m were estimated using the ENVI-met default configuration for the traffic distribution of the in-built traffic tool.

2.3.5. Data Analysis

The Leonardo tool in ENVI-met was used to extrapolate the PM2.5 concentration data. Given the focus of this study on roadside users' exposure to traffic-borne PM2.5 concentration, PM2.5 concentration data were extracted from vertical grid number three, which corresponds to the 1.4-m height of the 1:1 model scenario. The grid provides the closest match to pedestrians' breathing height. Horizontally, PM2.5 concentration was considered from both the leeward and windward sides of the urban roads. Figure 7 shows a schematic representation of the roadside user zone.

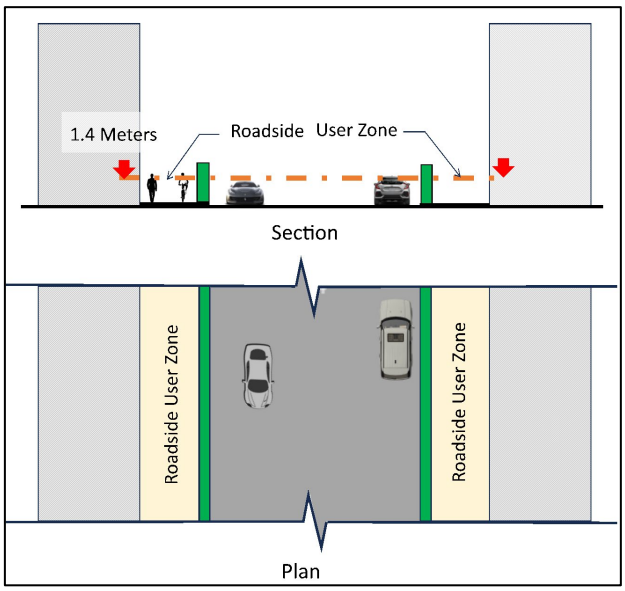

Figure 7. Schematic plan and section of the road model showing roadside user zone at the height of 1.4-m above the ground.

Data on the PM2.5 concentration were extrapolated for the base case as well as the four vegetation scenarios. All PM2.5 concentration data obtained from Leonardo were in micrograms per cubic meter ($\mu g/m^3$). PM2.5 concentrations on the roadsides were extrapolated from the 6th hour to the 22nd hour since ENVI-met requires the first few hours to achieve stability. The absolute percentage difference in PM2.5 between treeless urban road cases and scenarios with vegetation was calculated for the comparison.

The data obtained were analyzed using Spearman's rank correlation. The Spearman's rank correlation coefficient, commonly represented as r_s (rho), serves as a non-parametric statistical tool for evaluating the strength and direction of monotonic relationships between two variables [45]. Unlike Pearson correlation, which assumes a linear relationship, Spearman's rank correlation is based on the ranks of the data rather than their actual values. This makes it suitable for variables with non-linear associations or data that may not follow a normal distribution. Spearman's rank correlation assesses association, not causation [50].

The procedure entails assigning ranks to each variable's observations and converting the data into a set of ranks. The correlation coefficient is then calculated based on the differences between these ranks. A positive correlation coefficient indicates a monotonic increase in both variables, while a negative correlation coefficient suggests a monotonic decrease. The coefficient ranges from -1 to 1, where -1 represents a perfect negative correlation, 1 represents a perfect positive correlation, and 0 indicates no correlation.

3. Results

This section presents the results of simulations performed on Bank Street and Ali Bin Abi Talib Street. The impacts of the four vegetation scenarios, i.e., CH, SH, CT, and ST, on traffic-borne PM2.5 concentration in roadside user zones. Additionally, this section presents Spearman's rank correlation between PM2.5 concentration in the presence of the optimal vegetation scenarios in the roadside user zone and air temperature, humidity, and traffic-emitted PM2.5.

3.1. Bank Street

3.1.1. PM2.5 Concentration Reduction in Roadside User Zone

The line graph drawn (Figure 8) shows the temporal variations in PM2.5 concentration from 6 a.m. to 10 p.m. It reveals that SH shows lower PM2.5 concentrations than the base case from 8 a.m. to 4 p.m. However, the concentrations are higher during the early morning and evening hours compared to the base case. In the CH scenario, the temporal variations in PM2.5 concentrations do not differ much compared to the base-case scenario. The CT and ST scenarios showed higher PM2.5 concentrations throughout compared to the base case scenario and the ST scenario showed the highest PM2.5 concentrations.

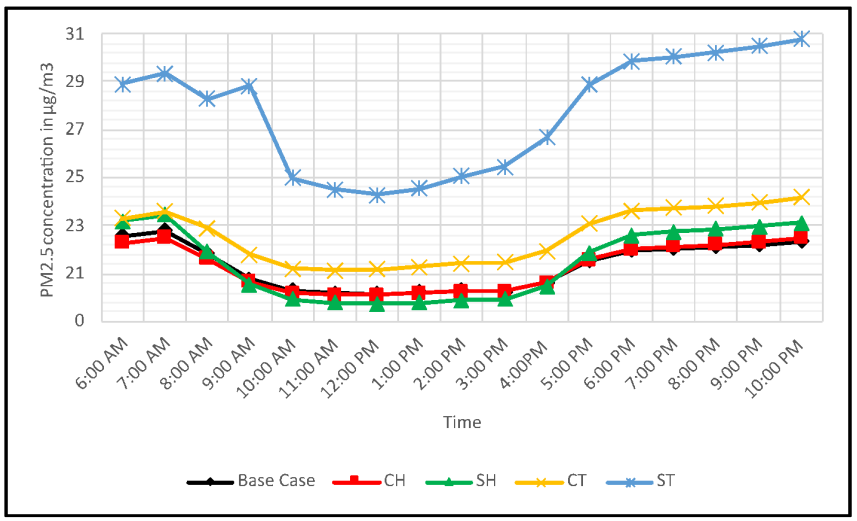

Figure 8. Temporal variations in PM2.5 concentrations in the five scenarios of the Bank Street models.

As shown in Figure 9, the boxplot illustrates the PM2.5 concentrations in the roadside user zone for the base case, CH, SH, CT, and ST scenarios. It shows that the median values of the base cases, CH, SH, CT, and ST, are 21.54, 21.57, 21.88, 22.90, and 28.83, respectively. The base-case scenario has the lowest median value compared to the vegetation scenarios. The mean values of base case, CH, SH, CT, and ST are 21.31, 21.26, 21.46, 22.57, and 27.71. For the SH scenario, the mean value is the lowest. It indicates that in most of the hours between 6 a.m. and 10 p.m., the base case scenario has the lowest PM2.5 concentration in roadside user zones; however, on average, the PM2.5 concentration is lower in the CH scenario compared to the base case scenario. The mean and median values for the ST scenario are the highest among all five scenarios. It shows that the ST scenario significantly increases the PM2.5 concentration in roadside user zones. Overall, CT and ST scenarios showed higher PM2.5 concentrations compared to CH and SH scenarios, with higher mean and median values.

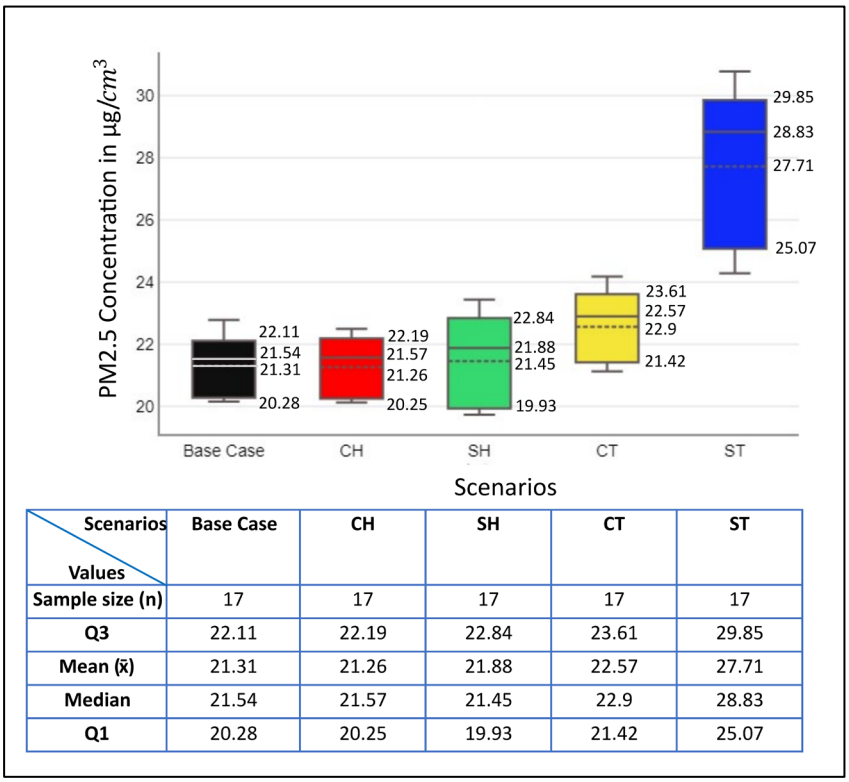

Scenarios / Values	Base Case	CH	SH	CT	ST
Sample size (n)	17	17	17	17	17
Q3	22.11	22.19	22.84	23.61	29.85
Mean ($\bar{x}$)	21.31	21.26	21.88	22.57	27.71
Median	21.54	21.57	21.45	22.9	28.83
Q1	20.28	20.25	19.93	21.42	25.07

Figure 9. Boxplot shows the effects of the four vegetation scenarios on traffic-borne PM2.5 concentration in roadside user zones in Bank Street.

3.1.2. Spearman's Rank Correlation between Air Temperature, Relative Humidity, Traffic Emission Rate, and the PM2.5 Concentration

Spearman's rank correlation was calculated between air temperature, relative humidity, traffic emission rate, and PM2.5 concentration in roadside user zones for the base case scenario and the four vegetation scenarios. Table 4 presents the results.

Spearman's rank correlation coefficients between the PM2.5 concentrations in the roadside user zones and air temperature is strongly associated with correlation coefficients of −0.98, −0.99, −0.95, −0.86, and −0.88 for the base case, CH, SH, CT, and ST scenarios, respectively. The results are statistically significant, with p-values less than 0.05 at a 95% confidence interval. It means that when the air temperature is higher, the PM2.5 concentration in the roadside user zone is lower, and when the air temperature is lower, the PM2.5 concentration in the roadside user zone is higher in the presence of CH.

Conversely, Spearman's rank correlation coefficient between the PM2.5 concentration and roadside user relative humidity is strong and positive, with correlation coefficients of

0.98, 0.99, 0.96, 0.89, and 0.90, respectively, for the base case, CH, SH, CT, and ST scenarios. The results are statistically significant, with *p*-values less than 0.05 at a 95% confidence interval. It means that when the relative humidity is higher, the PM2.5 concentration in the roadside user zone is also higher, whereas when the relative humidity is lower, the PM2.5 concentration in the roadside user zone is also lower in the presence of CH.

Table 4. Spearman's rank correlation (r_s) and significance (p) between PM2.5 concentration in roadside user zones in the five scenarios, air temperature and relative humidity, and traffic emission rate.

Variables	r_s and p	PM2.5 Concentration in Roadside User Zone				
		Base Case Scenario	CH Scenario	SH Scenario	CT Scenario	ST Scenario
Air Temperature [°C]	r_s	−0.98	−0.99	−0.95	−0.86	−0.88
	p	<0.001	<0.001	<0.001	<0.001	<0.001
Relative Humidity [%]	r_s	0.98	0.99	0.96	0.89	0.90
	p	<0.001	<0.001	<0.001	<0.001	<0.001
Traffic Emission Rate [µg/s]	r_s	−0.47	−0.44	−0.46	−0.37	−0.40
	p	0.06	0.07	0.06	0.14	0.11

For the base case, CH, SH, CT, and ST scenarios, the PM2.5 concentration in the roadside user zone weakly and negatively correlates with the traffic emission rate, with correlation coefficients of −0.47, −0.44, −0.46, −0.37, and −0.40, respectively. The results are not statistically significant, with *p*-values greater than 0.05 at a 95% confidence interval. It means that when the traffic emission rate is higher, the PM2.5 concentration in the roadside user zone is slightly lower, whereas when the traffic emission rate is lower, the PM2.5 concentration is slightly higher.

For the CH scenario, scatterplots were drawn to visualize Spearman's correlation coefficient between air temperature, relative humidity, traffic emission rate, and PM2.5 concentration in roadside user zones. Figure 10A displays scatter plots that correlate PM2.5 concentration rankings with air temperature rankings. Figure 10B displays a scatterplot correlating PM2.5 concentration rankings with relative humidity ranks. Figure 10C displays a scatterplot correlating PM2.5 concentration ranks with traffic emission rate ranks.

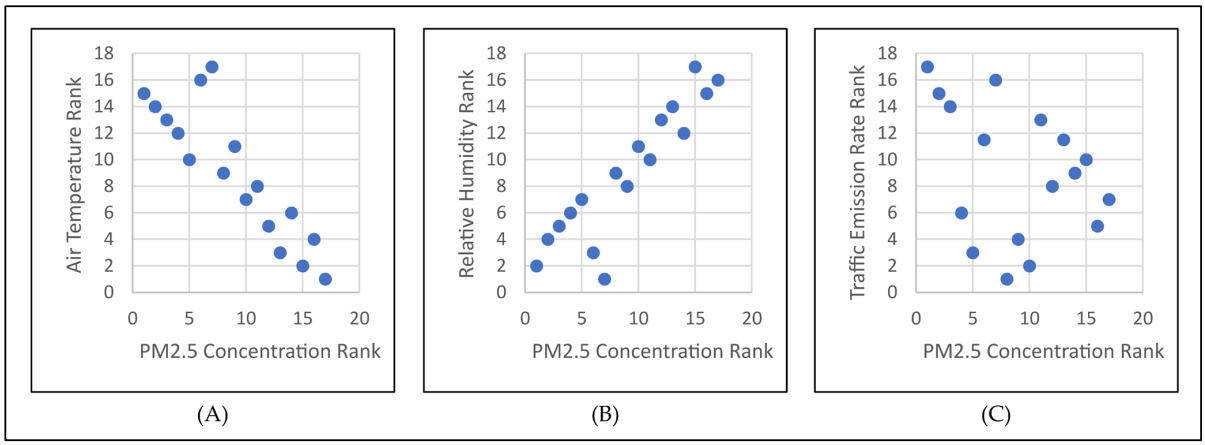

Figure 10. The scatterplot shows the rank distributions of PM2.5 concentration in the roadside user zone and air temperature (**A**), PM2.5 concentration in the roadside user zone and relative humidity (**B**), and PM2.5 concentration in the roadside user zone and traffic emission rate (**C**) in the Bank Street in CH scenario.

3.2. Ali Bin Abi Talib Street

3.2.1. PM2.5 Concentration Reduction in Roadside User Zone

The line graph drawn (Figure 11) shows the temporal variations in PM2.5 concentration from 6 a.m. to 10 p.m. It reveals that SH has lower PM2.5 concentrations than the

base case during the early morning and evening hours. However, the concentrations are higher from 8 a.m. to 4 p.m. compared to the base case. Temporal variations in the PM2.5 concentrations in the CH scenario do not vary much compared to the base case scenario; however, the concentrations are slightly higher than the base case scenario throughout. The CT and ST scenarios showed higher PM2.5 concentrations throughout compared to the base case scenario and the ST scenario showed the highest PM2.5 concentrations.

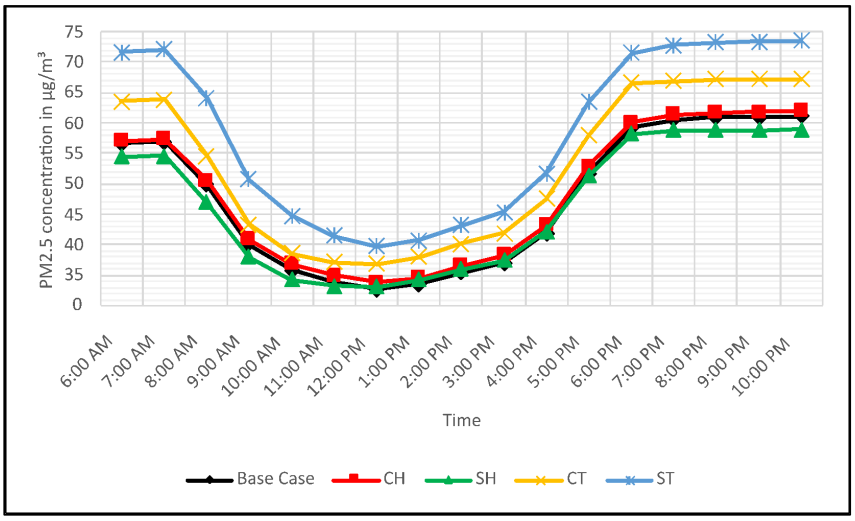

Figure 11. Temporal variations in PM2.5 concentrations in the five scenarios of Ali Bin Abi Talib Street models.

Boxplot analysis was conducted for the PM2.5 concentrations in roadside user zones in five scenarios, i.e., base case, CH, SH, CT, and ST, as shown in Figure 12.

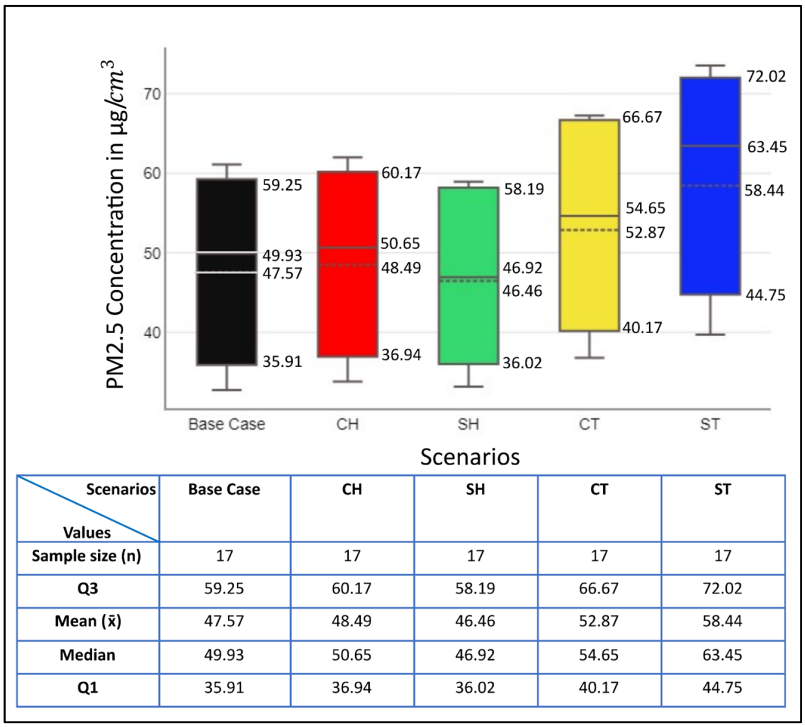

Scenarios / Values	Base Case	CH	SH	CT	ST
Sample size (n)	17	17	17	17	17
Q3	59.25	60.17	58.19	66.67	72.02
Mean (x̄)	47.57	48.49	46.46	52.87	58.44
Median	49.93	50.65	46.92	54.65	63.45
Q1	35.91	36.94	36.02	40.17	44.75

Figure 12. Boxplot shows the effects of the four vegetation scenarios on traffic-borne PM2.5 concentration in roadside user zones in Ali Bin Abi Talib Street.

The boxplot analysis shows that the median values of the base case, CH, SH, CT, and ST are 49.93, 50.65, 46.92, 54.65, and 63.45, respectively. The mean values of the base cases, CH, SH, CT, and ST are 47.57, 48.49, 46.46, 52.87, and 58.44. The median and mean values are the lowest for the SH scenario. It indicates that in most of the hours between 6 a.m. and 10 p.m., the SH scenario has the lowest PM2.5 concentration in roadside user zones and on average, PM2.5 concentration is lower in the SH scenario compared to the base case scenario. The mean and median values for the ST scenario are the highest among all five scenarios. It shows that the ST scenario significantly increases the PM2.5 concentration in roadside user zones. Overall, CT and ST scenarios showed higher PM2.5 concentrations compared to CH and SH scenarios, with higher mean and median values.

3.2.2. Spearman's Rank Correlation between Air Temperature, Relative Humidity, Traffic Emission Rate, and the PM2.5 Concentration

Spearman's rank correlation was calculated between PM2.5 concentration in the roadside user zone in the presence of SH, air temperature and relative humidity, and traffic emission rate. Table 5 presents the results.

Table 5. Spearman's rank correlation (r_s) and significance (p) between PM2.5 concentration in roadside user zones in the presence of SH, air temperature and relative humidity, and traffic emission rate.

Variables	r_s and p	PM2.5 Concentrations in Roadside User Zones				
		Base Case Scenario	CH Scenario	SH Scenario	CT Scenario	ST Scenario
Air Temperature [°C]	r_s	−0.89	−0.89	−0.88	−0.88	−0.93
	p	<0.001	<0.001	<0.001	<0.001	<0.001
Relative Humidity [%]	r_s	0.91	0.91	0.90	0.90	0.94
	p	<0.001	<0.001	<0.001	<0.001	<0.001
Traffic Emission Rate [µg/s]	r_s	−0.34	−0.34	−0.36	−0.36	−0.40
	p	0.18	0.18	0.154	0.15	0.11

Scatterplots were drawn to visualize the Spearman's correlation coefficients between the PM2.5 concentrations in the roadside user zones, and air temperature. It shows that the PM2.5 concentrations are strongly and negatively correlated with air temperature, with correlation coefficients of −0.89, −0.89, −0.88, −0.88, and −0.93 for the base case, CH, SH, CT, and ST scenarios, respectively. The results are statistically significant, with *p*-values less than 0.05 at a 95% confidence interval. It means that in the presence of SH, when the air temperature is higher, the PM2.5 concentration in the roadside user zone is lower and when the air temperature is lower, the PM2.5 concentration in the roadside user zone is higher.

Conversely, for the base case, CH, SH, CT, and ST scenarios, the Spearman's rank correlation coefficient between the PM2.5 concentration in the roadside user zone and relative humidity is strongly and positively correlated, with correlation coefficients of 0.91, 0.91, 0.9, 0.9, and 0.94, respectively. The results are statistically significant, with *p*-values less than 0.05 at a 95% confidence interval. It means that when the relative humidity is higher, the PM2.5 concentration in the roadside user zone is also higher, whereas when the relative humidity is lower, the PM2.5 concentration in the roadside user zone is also lower.

The traffic emission rate and PM2.5 concentration in the roadside user zone have a moderately negative correlation, with correlation coefficients of −0.34, −0.34, −0.36, and −0.40, respectively. However, the results are statistically not significant, with *p*-values greater than 0.05 at a 95% confidence interval. This means that when the traffic emission rate is higher, the PM2.5 concentration in the roadside user zone is slightly lower, whereas when the traffic emission rate is lower, the PM2.5 concentration is slightly higher.

For the SH scenario, scatterplots were drawn to visualize Spearman's correlation coefficient between air temperature, relative humidity, traffic emission rate, and PM2.5 concentration in roadside user zones. Figure 13A displays scatter plots correlating PM2.5 concentration rankings with air temperature ranks. Figure 13B displays a scatterplot

correlating PM2.5 concentration rankings with relative humidity ranks. Figure 13C displays a scatterplot correlating PM2.5 concentration ranks with traffic emission rate ranks.

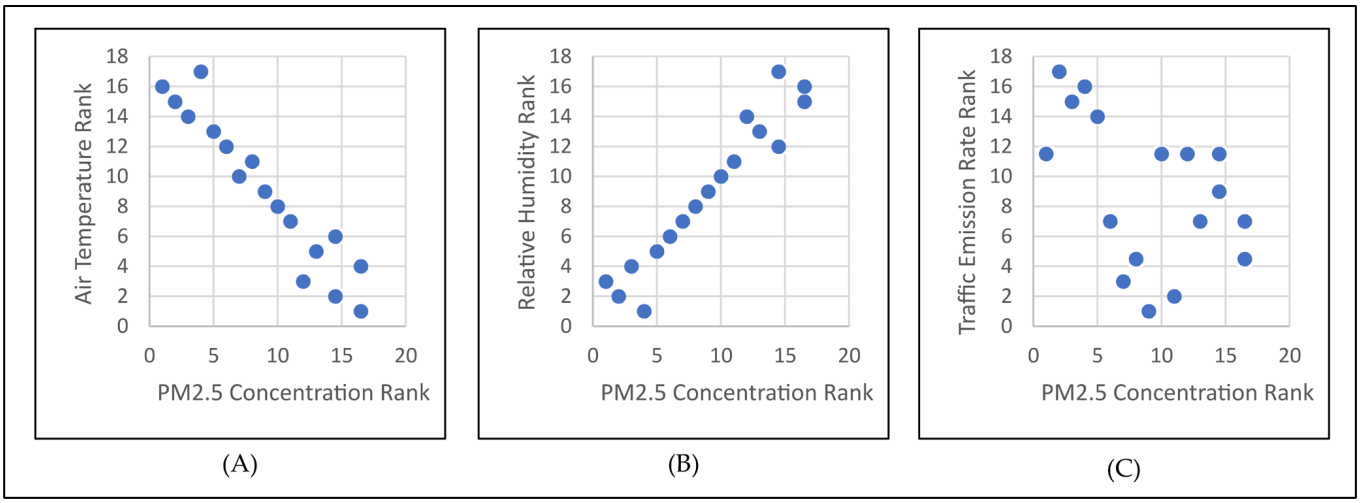

Figure 13. The scatter plot shows the rank distributions of PM2.5 concentration in the roadside user zone and air temperature (**A**), PM2.5 concentration in the roadside user zone and relative humidity (**B**), and PM2.5 concentration in the roadside user zone and traffic emission rate (**C**) in Ali Bin Abi Talib Street in SH scenario.

4. Discussion

The research looked at how four common types of road vegetation—CH, SH, CT, and ST—affected the amount of PM2.5 that was carried by traffic in two streets in central Doha, Qatar: Bank Street and Ali Bin Abi Talib Street. It also examined the influences of air temperature, relative humidity, and traffic emission rate on the PM2.5 concentration in roadside user zones in the presence and absence of vegetation scenarios.

According to the results, the PM2.5 concentration in Ali Bin Abi Talib Street is much higher than that in Bank Street. The primary distinctions between the two road models lie in the total volume the road occupies and the orientation of the road relative to the prevailing wind direction. According to the literature, the pollutant concentration in roadside areas is significantly higher on a road oriented at 75° than on a road oriented at 45° to the prevailing wind direction. It is also a well-known fact that as volume increases, pollutant concentration dilutes.

The CH scenario on Bank Street, oriented at 46° to the prevailing wind direction, is evident in the results. Zhang et al. [20] demonstrated, as previously mentioned, that sidewise vegetation arrangement is appropriate for urban roads oriented parallel to and perpendicular to the wind. The street aspect ratio is the main difference between this study and Zhang et al. [20]. Zhang et al. [20] applied a street aspect ratio of 1, while this study applied a ratio of 0.5. It indicates that the effects of vegetation on PM2.5 concentrations in roadside user zones also vary according to aspect ratios. In this study, both roads exhibit an oblique tilt toward the prevailing wind direction, albeit at varying angles. The study found that Ali Bin Abi Talib Street, oriented at 75° to the prevailing wind direction, is the most suitable for reducing PM2.5 concentration. It indicates that within the obliquely oriented roads to the prevailing wind direction, differences in the angles can have a substantial influence on vegetation effects on PM2.5 concentration in roadside user zones.

The temporal variation in the PM2.5 concentrations in the roadside user zone showed that the CH scenario effectively reduced the concentrations from 8 a.m. to 4 p.m. on Bank Street. In Ali Bin Abi Talib Street, the SH scenario reduced the concentration during the early morning and evening hours. It suggests that the effects of air temperature and relative humidity on vegetation and PM2.5 concentration may vary over time.

Results show that trees (CT and ST) consistently increase PM2.5 concentration in both streets and the ST scenario appears to show the highest increase. Other studies, such as those by Buccolieri et al. [13] and Gromke and Ruck [14], also showed a similar result for ST. Hedgerows (CH and SH) showed better performance than trees. This is primarily because hedgerows impede wind velocity in street canyons less than trees, thereby contributing more to pollution dispersion [19].

The results revealed that in all five scenarios, air temperature has a robust negative correlation with PM2.5 concentration in roadside user zones, while relative humidity has a robust positive correlation. It indicates that as the air temperature increases, the PM2.5 concentration decreases while increasing with an increase in relative humidity. Therefore, we can anticipate an increase in PM2.5 concentrations in roadside user zones during cooler months with higher relative humidity. On the other hand, we can anticipate a decrease in PM2.5 concentrations during the hotter months with lower relative humidity.

Previously, studies such as Sini et al. [35], Baik and Kim [34], and Xie et al. [33] showed that airflow regimes in street canyons of various aspect ratios change with an increase in surface heating and influence traffic-borne pollutant dispersion. Particularly, regarding the aspect ratio of 0.5, Xie et al. [33] revealed that the spatial behaviors of air pollutant movement in the street canyon were similar in wall and ground heating scenarios. The heating scenarios formed two vertices, comprising a primary vortex that extended beyond the roof level and a secondary vortex positioned at the windward corner at ground level. The pollutants were carried toward the leeward side shortly after being emitted from the source. Consequently, pollutant concentration increased at the leeward wall side, which was then uplifted along the leeward wall by the primary vortex, and the pollutant gradually dissipated or re-entered the street canyon at the roof level. In summary, the surface heating scenarios strengthened the primary vertex, shifted pollutants upward along the leeward wall, and gradually dissipated the pollutants.

Studies have shown that relative humidity plays an important role in the dispersion and dry deposition of particulate matter in relation to relative humidity [51,52]. Previously, Chen et al. [31] in Wuhan, China, reported that the sizes of hygroscopic particles grow with an increase in relative humidity, which impedes particle movement, thus increasing particulate matter concentration in the form of haze. On average, over 70% of RH and 28% of no-wind weather occur in Wuhan each year. A gray relational analysis of air temperature, relative humidity, and wind speed revealed that relative humidity significantly influences the efficiency of vegetation-induced particulate matter removal. The study showed that relative humidity has the greatest impact on vegetation-induced particulate matter reduction in roadside user zones. In general, as the wind velocity increases, the rate of particle diffusion accelerates. An increase in relative humidity facilitates the condensation of airborne particles, making a significant contribution to the formation of fog and haze. Due to the Brownian motion of particles, temperature has a less significant impact on particulate removal efficiency in regions with lower wind speeds than relative humidity or wind speed [53]. Compared to Wuhan, the wind speed in Doha is much higher, with a yearly average wind speed of 3.76 m/s. Therefore, wind speed might have played a role in having an almost equal influence of both air temperature and relative humidity on the PM2.5 dispersion in roadside user zones in this study.

Finally, this study showed a moderate and negative correlation between the PM2.5 concentration in the roadside user zone and traffic emission rate. However, we found no statistical significance in the correlation. It indicates that road vegetation's benefit in reducing the average concentration of PM2.5 in roadside user zones may be greater on roads with higher vehicular traffic flow. Since the correlation is not statistically significant, further investigations are necessary.

To summarize, this study provides the following insights into road vegetation design in central Doha

- Hedgerows have the potential to reduce roadside users' exposure to traffic-borne PM2.5;

- Trees significantly increase the PM2.5 concentrations in roadside user zones;
- Air temperature and relative humidity both have a significant influence on the PM2.5 concentration in the roadside user zone. In the roadside user zone, the air temperature is negative, while relative humidity is positively associated with the PM2.5 concentration;
- Traffic emissions may have a moderate influence on the PM2.5 concentration in the roadside user zone;
- The influence of air temperature and relative humidity on the PM2.5 concentration in roadside user zones does not differ substantially in the presence of vegetation;
- The influence of air temperature and relative humidity on the PM2.5 concentration may vary slightly depending on wind directions.

Overall, this study successfully demonstrated that the road's orientation to the prevailing wind direction plays a crucial role in the selection of vegetation to reduce traffic-borne PM2.5 exposure for roadside users. It also showed that air temperature and relative humidity both have a significant influence on vegetation effects on PM2.5 concentration in roadside user zones in the local climate. In general, in all five scenarios, i.e., base-case, CH, SH, CT, and ST, traffic-borne PM2.5 concentration is lowest when the air temperature is the highest and the relative humidity is the lowest.

However, this study has limitations in several areas. Firstly, the roads selected for the case study are the same in terms of aspect ratio but different in the volume occupied. Secondly, we assumed the AADT during the modeling process due to the lack of readily available data. Thirdly, the LAD of trees and hedgerows was assumed based on the literature. Finally, this study confines itself to the four prevalent vegetation scenarios.

5. Conclusions

This study revealed the applicability of the four common road vegetation scenarios in reducing roadside users' exposure to traffic-borne PM2.5 concentrations. It revealed that hedgerows are more effective than trees in reducing the PM2.5 concentration in roadside user zones. Trees have the potential to significantly increase the concentration in the roadside user zone. Both air temperature and relative humidity have a robust correlation with the PM2.5 concentration in roadside user zones. Vegetation might be beneficial in reducing roadside user exposure to traffic-borne PM2.5 concentrations on heavy-traffic roads.

Future research endeavors can assess the impact of vegetation on traffic-borne PM2.5 concentrations across varying wind directions. Furthermore, we can conduct investigations in various geographical locations, as microclimate and street geometry have the potential to influence the effects of vegetation on the PM2.5 concentrations in roadside user zones. Additionally, we can conduct investigations on various arrangements and sizes of urban road vegetation to identify the most effective configurations for pollutant reduction. By systematically investigating these aspects, future studies can contribute valuable knowledge to inform the design and implementation of vegetation-based strategies for improving air quality in roadside user zones.

Supplementary Materials: The following supporting information can be downloaded at https://www.mdpi.com/article/10.3390/buildings14051388/s1. Figure S1: Base Case Model with grid resolution 3.6 m × 3.6 m × 2 m modeled using ENVI-met, Figure S2: Model with Avenue Trees with grid resolution 3.6 m × 3.6 m × 2 m modeled using ENVI-met, Table S1: ENVI-met simulation file input values for relative humidity (RH) and air temperature.

Author Contributions: Conceptualization, S.M. and M.F.K.; methodology, S.M. and M.F.K.; software, S.M.; validation, S.M.; formal analysis, S.M. and M.F.K.; investigation, S.M. and M.F.K.; resources, S.M. and M.F.K.; data curation, S.M.; writing—S.M.; writing—review and editing, S.M. and M.F.K.; visualization, S.M. and M.F.K.; supervision, M.F.K.; project administration, S.M. and M.F.K. All authors have read and agreed to the published version of the manuscript.

Funding: This research received no specific grant from any funding agency in the public, commercial, or not-for-profit sector.

Data Availability Statement: The dataset of the study is available from the author upon reasonable request.

Conflicts of Interest: The authors declare that there are no conflicts of interest.

References

1. WHO. Ambient (Outdoor) Air Quality and Health. Fact Sheet. 2018. Available online: https://www.who.int/en/news-room/fact-sheets/detail/ambient-(outdoor)-air-quality-and-health (accessed on 4 April 2024).
2. World Health Organization. Concentration of Fine Particulate Matter (PM2.5). 2022. Available online: https://www.who.int/data/gho/data/indicators/indicator-details/GHO/concentrations-of-fine-particulate-matter-(pm2-5) (accessed on 4 April 2024).
3. United States Environmental Protection Agency. Particulate Matter (PM) Basics. 2024. Available online: https://www.epa.gov/pm-pollution/particulate-matter-pm-basics (accessed on 6 April 2024).
4. IQAir. Air Quality in Qatar: Air Quality Index and PM2.5 Air Pollution in Qatar. 2024. Available online: https://www.iqair.com/qa/qatar (accessed on 24 April 2024).
5. United States Environmental Protection Agency. Revised Air Quality Standards for Particle Pollution and Updates to the Air Quality Index (AQI). 2024. Available online: https://www.epa.gov/sites/default/files/2016-04/documents/2012_aqi_factsheet.pdf (accessed on 24 April 2024).
6. Javed, W.; Iakovides, M.; Garaga, R.; Stephanou, E.G.; Kota, S.H.; Ying, Q.; Wolfson, J.M.; Koutrakis, P.; Guo, B. Source apportionment of organic pollutants in fine and coarse atmospheric particles in Doha, Qatar. *J. Air Waste Manag. Assoc.* **2019**, *69*, 1277–1292. [CrossRef] [PubMed]
7. Javed, W.; Guo, B. Chemical characterization and source apportionment of fine and coarse atmospheric particulate matter in Doha, Qatar. *Atmos. Pollut. Res.* **2021**, *12*, 122–136. [CrossRef]
8. Al-Thani, H.; Koc, M.; Isaifan, R.J. Investigations on Deposited Dust Fallout in Urban Doha: Characterization, Source Apportionment and Mitigation. *Environ. Ecol. Res.* **2018**, *6*, 493–506. [CrossRef]
9. Abhijith, K.V.; Kumar, P.; Gallagher, J.; McNabola, A.; Baldauf, R.; Pilla, F.; Broderick, B.; Di Sabatino, S.; Pulvirenti, B. Air pollution abatement performances of green infrastructure in open road and built-up street canyon environments—A review. *Atmos. Environ.* **2017**, *162*, 71–86. [CrossRef]
10. Vardoulakis, S.; Fisher, B.E.A.; Pericleous, K.; Gonzalez-Flesca, N. Modelling air quality in street canyons: A review. *Atmos. Environ.* **2003**, *37*, 155–182. [CrossRef]
11. Janhäll, S. Review on urban vegetation and particle air pollution–Deposition and dispersion. *Atmos. Environ.* **2015**, *105*, 130–137. [CrossRef]
12. Garland, J.A. On the Size Dependence of Particle Deposition. *Water Air Soil Pollut. Focus* **2001**, *1*, 323–332. [CrossRef]
13. Buccolieri, R.; Gromke, C.; Di Sabatino, S.; Ruck, B. Aerodynamic effects of trees on pollutant concentration in street canyons. *Sci. Total Environ.* **2009**, *407*, 5247–5256. [CrossRef]
14. Gromke, C.; Ruck, B. Pollutant Concentrations in Street Canyons of Different Aspect Ratio with Avenues of Trees for Various Wind Directions. *Bound.-Layer Meteorol.* **2012**, *144*, 41–64. [CrossRef]
15. Huang, Y.-D.; Hou, R.-W.; Liu, Z.-Y.; Song, Y.; Cui, P.-Y.; Kim, C.-N. Effects of Wind Direction on the Airflow and Pollutant Dispersion inside a Long Street Canyon. *Aerosol Air Qual. Res.* **2019**, *19*, 1152–1171. [CrossRef]
16. Li, X.-B.; Lu, Q.-C.; Lu, S.-J.; He, H.-D.; Peng, Z.-R.; Gao, Y.; Wang, Z.-Y. The impacts of roadside vegetation barriers on the dispersion of gaseous traffic pollution in urban street canyons. *Urban For. Urban Green.* **2016**, *17*, 80–91. [CrossRef]
17. Wang, J.; Gao, H.; Lv, C. Analysing the influence of different street vegetation on particulate matter dispersion using microscale simulations. *Desalin. Water Treat.* **2018**, *110*, 319–327. [CrossRef]
18. Zhu, X.; Wang, X.; Lei, L.; Zhao, Y. The influence of roadside green belts and street canyon aspect ratios on air pollution dispersion and personal exposure. *Urban Clim.* **2022**, *44*, 101236. [CrossRef]
19. Wania, A.; Bruse, M.; Blond, N.; Weber, C. Analysing the influence of different street vegetation on traffic-induced particle dispersion using microscale simulations. *J. Environ. Manag.* **2012**, *94*, 91–101. [CrossRef] [PubMed]
20. Zhang, L.; Zhang, Z.; Feng, C.; Tian, M.; Gao, Y. Impact of various vegetation configurations on traffic fine particle pollutants in a street canyon for different wind regimes. *Sci. Total Environ.* **2021**, *789*, 147960. [CrossRef]
21. Gromke, C.; Ruck, B. Influence of trees on the dispersion of pollutants in an urban street canyon—Experimental investigation of the flow and concentration field. *Atmos. Environ.* **2007**, *41*, 3287–3302. [CrossRef]
22. Huang, Y.-D.; Li, M.-Z.; Ren, S.-Q.; Wang, M.-J.; Cui, P.-Y. Impacts of tree-planting pattern and trunk height on the airflow and pollutant dispersion inside a street canyon. *Build. Environ.* **2019**, *165*, 106385. [CrossRef]
23. Zhang, L.; Zhang, Z.; McNulty, S.; Wang, P. The mitigation strategy of automobile generated fine particle pollutants by applying vegetation configuration in a street-canyon. *J. Clean. Prod.* **2020**, *274*, 122941. [CrossRef]

24. Shen, J.; Cui, P.; Huang, Y.; Wu, Y.; Luo, Y.; Sin, C.H.; Guan, J. New insights on precise regulation of pollutant distribution inside a street canyon by different vegetation planting patterns. *Environ. Sci. Pollut. Res.* **2023**, *30*, 63148–63174. [CrossRef]
25. Buccolieri, R.; Salim, S.M.; Leo, L.S.; Di Sabatino, S.; Chan, A.; Ielpo, P.; de Gennaro, G.; Gromke, C. Analysis of local scale tree-atmosphere interaction on pollutant concentration in idealized street canyons and application to a real urban junction. *Atmos. Environ.* **2011**, *45*, 1702–1713. [CrossRef]
26. Vos, P.; Maiheu, B.; Vankerkom, J.; Janssen, S. Improving local air quality in cities: To tree or not to tree? *Environ. Pollut.* **2013**, *144*, 41–64. [CrossRef] [PubMed]
27. Morakinyo, T.E.; Lam, Y.F. Study of traffic-related pollutant removal from street canyon with trees: Dispersion and deposition perspective. *Environ. Sci. Pollut. Res.* **2016**, *23*, 21652–21668. [CrossRef] [PubMed]
28. Amorim, J.H.; Rodrigues, V.; Tavares, R.; Valente, J.; Borrego, C. CFD modelling of the aerodynamic effect of trees on urban air pollution dispersion. *Sci. Total Environ.* **2013**, *461–462*, 541–551. [CrossRef] [PubMed]
29. Gromke, C.; Jamarkattel, N.; Ruck, B. Influence of roadside hedgerows on air quality in urban street canyons. *Atmos. Environ.* **2016**, *139*, 75–86. [CrossRef]
30. Hong, B.; Lin, B.; Qin, H. Numerical Investigation on the Effect of Avenue Trees on PM2.5 Dispersion in Urban Street Canyons. *Atmosphere* **2017**, *8*, 129. [CrossRef]
31. Chen, X.; Pei, T.; Zhou, Z.; Teng, M.; He, L.; Luo, M.; Liu, X. Efficiency differences of roadside greenbelts with three configurations in removing coarse particles (PM_{10}): A street scale investigation in Wuhan, China. *Urban For. Urban Green.* **2015**, *14*, 354–360. [CrossRef]
32. Vranckx, S.; Vos, P.; Maiheu, B.; Janssen, S. Impact of trees on pollutant dispersion in street canyons: A numerical study of the annual average effects in Antwerp, Belgium. *Sci. Total Environ.* **2015**, *532*, 474–483. [CrossRef] [PubMed]
33. Xie, X.; Liu, C.-H.; Leung, D.Y.C. Impact of building facades and ground heating on wind flow and pollutant transport in street canyons. *Atmos. Environ.* **2007**, *41*, 9030–9049. [CrossRef]
34. Baik, J.-J.; Kim, J.-J. A Numerical Study of Flow and Pollutant Dispersion Characteristics in Urban Street Canyons. *J. Appl. Meteorol.* **1999**, *38*, 1576–1589. [CrossRef]
35. Sini, J.-F.; Anquetin, S.; Mestayer, P.G. Pollutant dispersion and thermal effects in urban street canyons. *Atmos. Environ.* **1996**, *30*, 2659–2677. [CrossRef]
36. Baik, J.-J.; Park, R.-S.; Chun, H.-Y.; Kim, J.-J. A Laboratory Model of Urban Street-Canyon Flows. *J. Appl. Meteorol.* **2000**, *39*, 1592–1600. [CrossRef]
37. Mogra, S.; Khamidi, M.F.; Fadli, F. Insight into vegetation inclusion along urban roads: A pilot study on the preferences of expatriate roadside users in downtown Doha, Qatar. *Landsc. Online* **2023**, *98*, 1108. [CrossRef]
38. QNMP. *Qatar Urban Design Compendium (QUDC)*; QNMP: Doha, Qatar, 2019.
39. Sun, D.; Wu, S.; Shen, S.; Xu, T. Simulation and assessment of traffic pollutant dispersion at an urban signalized intersection using multiple platforms. *Atmos. Pollut. Res.* **2021**, *12*, 101087. [CrossRef]
40. PSA. *Residence for Households by Zone 2020*; PSA: Doha, Qatar, 2020; Available online: https://psaqatar.maps.arcgis.com/apps/dashboards/4e2cf1451a8f43c2b258751609752cae (accessed on 24 April 2024).
41. Bruse, M. ENVI-Met Implementation of the Gas/Particle Dispersion and Deposition Model PDDM. 2007. Available online: http://envi-met.com/documents/sources (accessed on 24 April 2024).
42. Abhijith, K.V.; Gokhale, S. Passive control potentials of trees and on-street parked cars in reduction of air pollution exposure in urban street canyons. *Environ. Pollut.* **2015**, *204*, 99–108. [CrossRef]
43. Buccolieri, R.; Jeanjean, A.P.R.; Gatto, E.; Leigh, R.J. The impact of trees on street ventilation, NO_x and $PM_{2.5}$ concentrations across heights in Marylebone Rd street canyon, central London. *Sustain. Cities Soc.* **2018**, *41*, 227–241. [CrossRef]
44. Jeanjean, A.P.R.; Hinchliffe, G.; McMullan, W.A.; Monks, P.S.; Leigh, R.J. A CFD study on the effectiveness of trees to disperse road traffic emissions at a city scale. *Atmos. Environ.* **2015**, *120*, 1–14. [CrossRef]
45. Jeanjean, A.P.R.; Buccolieri, R.; Eddy, J.; Monks, P.S.; Leigh, R.J. Air quality affected by trees in real street canyons: The case of Marylebone neighbourhood in central London. *Urban For. Urban Green.* **2017**, *22*, 41–53. [CrossRef]
46. CODASC. CODASC Laboratory of Building-and Environmental Aerodynamics Karlsruhe Institute of Technology KIT. Available online: https://www.umweltaerodynamik.de/bilder-originale/CODA/CODASC.html (accessed on 16 November 2023).
47. Chang, J.C.; Hanna, S. *Technical Descriptions and User's Guide for the BOOT Statistical Model Evaluation Software Package, Version 2.0*; George Mason University and Harvard School of Public Health: Fairfax, VA, USA, 2005.
48. IEM. Computed Daily Summary of Observations. 2023. Available online: https://mesonet.agron.iastate.edu/request/daily.phtml?network=QA__ASOS (accessed on 24 September 2023).
49. National Research Council; Transportation Research Board. *Highway Capacity Manual: A Guide for Multimodal Mobility Analysis*, 6th ed.; Transportation Research Board: Washington, DC, USA, 2016.
50. Dodge, Y. Spearman Rank Correlation Coefficient. In *The Concise Encyclopedia of Statistics*; Springer: New York, NY, USA, 2008; pp. 502–505. [CrossRef]

51. Chen, L.; Peng, S.; Liu, J.; Hou, Q. Dry deposition velocity of total suspended particles and meteorological influence in four locations in Guangzhou, China. *J. Environ. Sci.* **2012**, *24*, 632–639. [CrossRef]
52. Zhang, M.; Chen, S.; Zhang, X.; Guo, S.; Wang, Y.; Zhao, F.; Chen, J.; Qi, P.; Lu, F.; Chen, M.; et al. Characters of Particulate Matter and Their Relationship with Meteorological Factors during Winter Nanyang 2021–2022. *Atmosphere* **2023**, *14*, 137. [CrossRef]
53. Dimbour, J.P.; Dandrieux, A.; Dusserre, G. Reduction of chlorine concentrations by using a greenbelt. *J. Loss Prev. Process Ind.* **2002**, *15*, 329–334. [CrossRef]